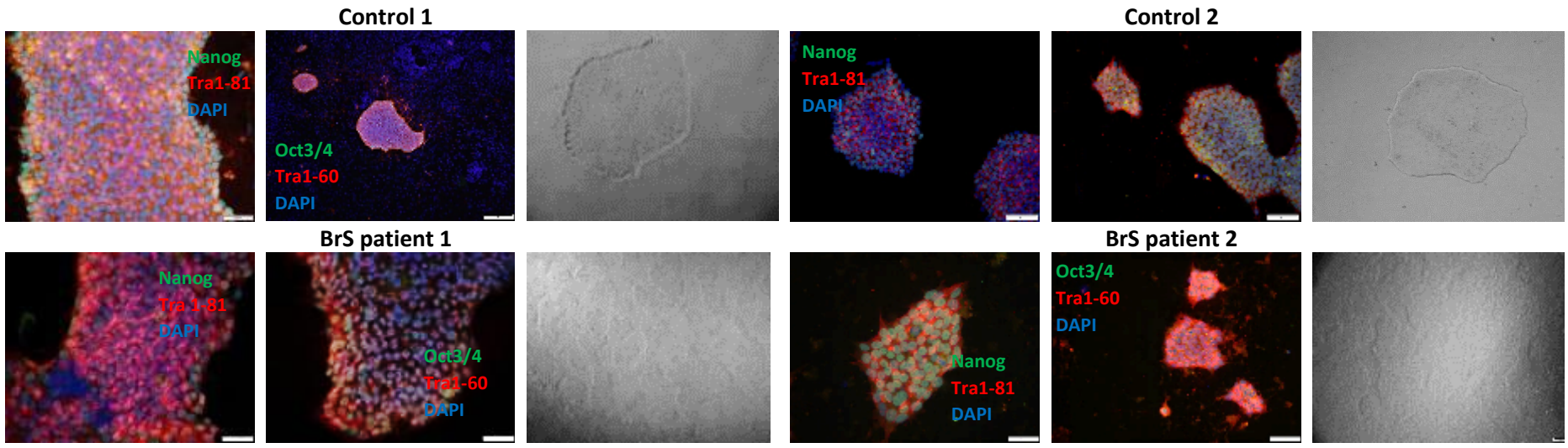

Fig. S1. Bright field images and representative immunofluorescence staining of pluripotency markers of iPSCs of Control 1, Control 2, BrS patient 1 and BrS patient 2.

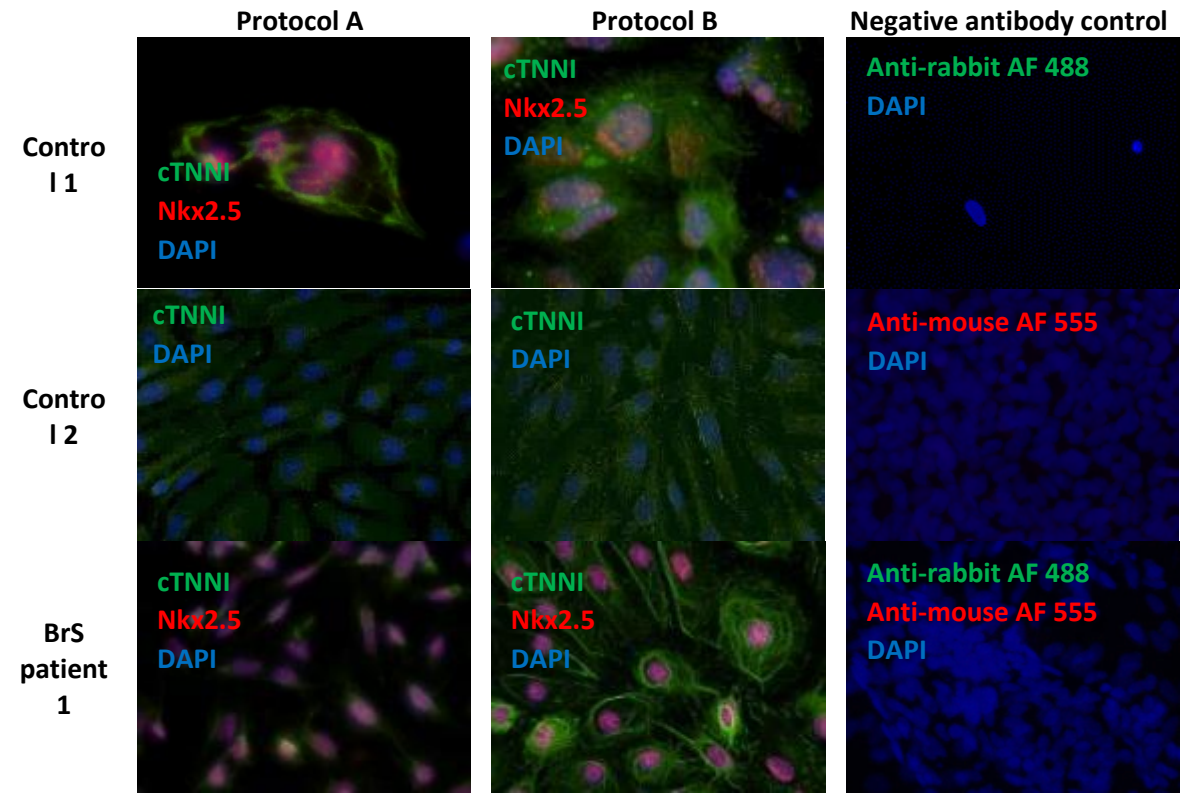

Fig. S2. Immunofluorescence staining of cTNNI of iPSC-CMs of Control 1, 2 and BrS patient 1 generated with protocol A and B in the comparison experiment. No cTNNI or Nkx2.5 staining was performed on iPSC-CMs from BrS patient 2 due to low amount of contracting areas on coverslips, which were used for electrophysiological tests and ICC staining for cACT. Negative secondary antibody controls (anti-rabbit Alexa Fluor 488 and/or anti-mouse Alexa Fluor 555) are shown in the right column.

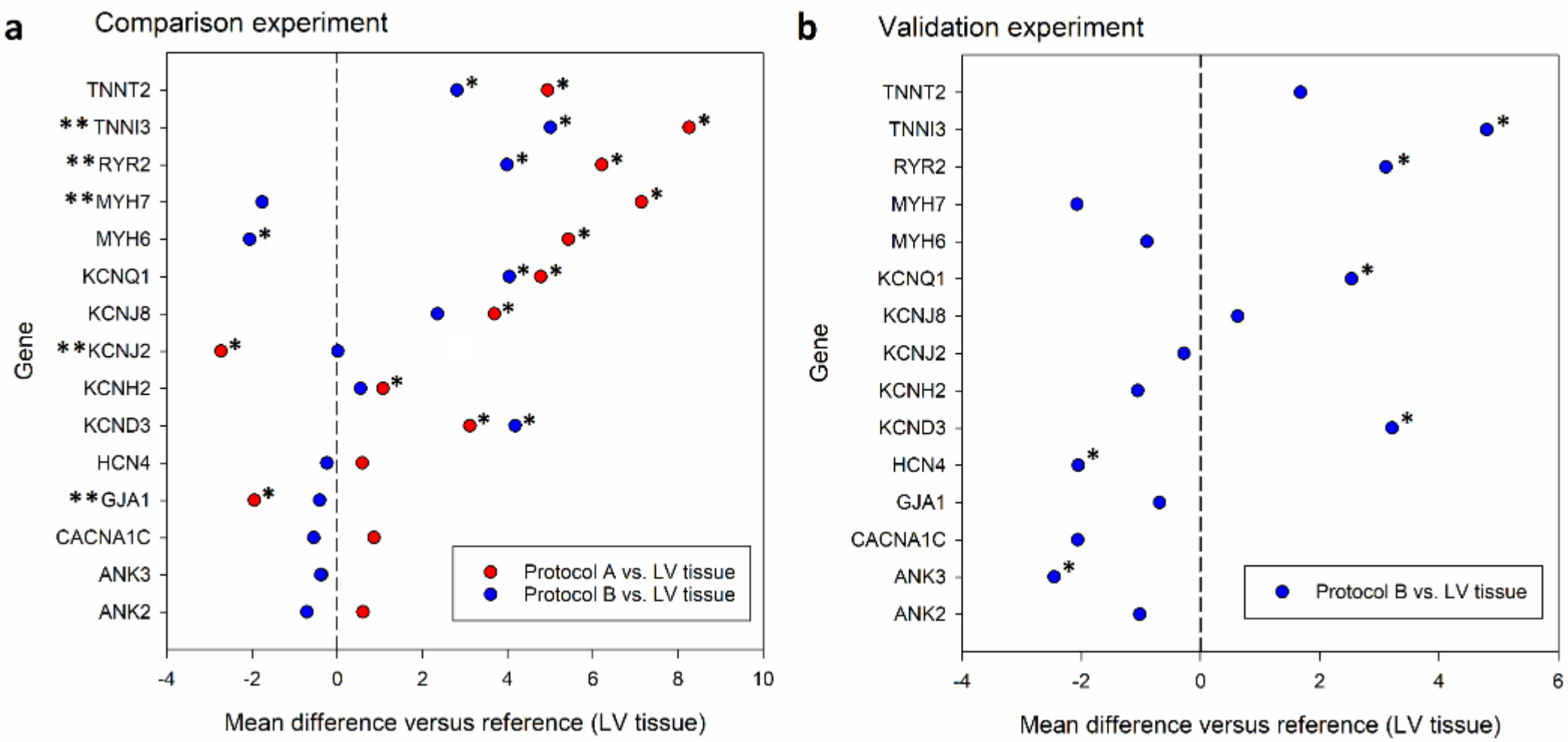

Fig. S3. Measured Ct values for all tested genes in iPSC-CMs generated using protocol A (in red) and protocol B (in blue) in relation to left ventricle (0 level on the x axis) from samples obtained in the comparison (a) and validation (b) experiment.
The figures show graphical overview of the difference in the measured mean Ct values. Values for iPSC-CMs generated with protocol B in comparison experiment show closer resemblance to those in the reference tissue in comparison to iPSC-CMs generated with protocol A. $^{*}p \leq 0.05$ for Ct comparison between the used protocol versus reference tissue (left ventricle of the healthy donor heart); $^{**}p \leq 0.05$ for Ct comparison between protocols A and B.

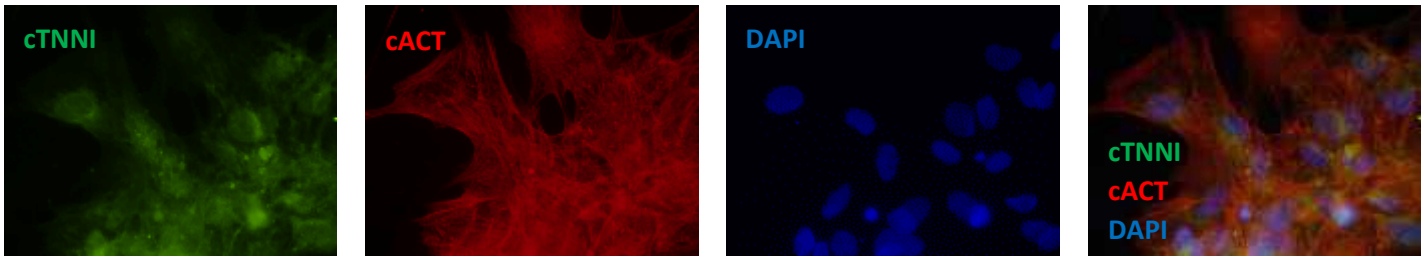

Fig. S4. Unmerged immunofluorescence staining images of cardiac markers cACT and cTNNI obtained from iPSC-CMs in the validation experiment (merged images are presented in Fugure 4a).

Table S1. CNVs (larger than 100kb) detected in the used iPSC-lines.

Cell line	CNV type	CNV minimal region	CNV size (bp)	Genes in the region
Control 1	del	Chr1:1,030,565-1,266,041	235477	ACAP3, mir429, TTLL10
	del	Chr1:2,532,899-2,745,883	212985	MMEL1
	del	Chr1:191,618,129-191,875,752	257624	
	del	Chr4:994,414-1,188,049	193636	FGFRL1
	del	Chr4:34,049,908-34,423,079	373172	LINC02484
	del	Chr4:43,363,694-43,526,808	163115	LINC02383
	del	Chr4:113,294,328-113,779,891	485564	ALPK1, mir367
	del	Chr6:27,002,406-27,194,072	191667	HIST1H2AG
	del	Chr8:78,359,134-78,510,649	151516	LOC102724874
	del	Chr8:144,669,392-144,861,985	192594	BREA2, PYCR3
	del	Chr8:144,998,779-145,268,000	269222	CYC1, MROH1
	dup	Chr10:54,002,021-54,141,652	139632	DKK1
	del	Chr11:39,066,761-39,266,095	199335	
	del	Chr14:105,285,159-105,395,204	110046	CEP170B
	del	Chr19:1,341,509-1,497,060	155552	APC2
	del	Chr19:1,566,043-1,712,898	146856	MBD3
	dup	ChrX:71,284,941-71,411,659	126719	FLI44635
	dup	ChrX:91,685,124-92,178,902	493779	PCDH11X
Control 2	del	Chr16:32,624,879-32,855,389	230511	TP53TG3
	dup	Chr19:54,737,010-54,841,732	104723	LILRA3
	dup	ChrX:48,645,256-48,746,726	101471	ERAS
	dup	ChrX:153,051,907-153,197,130	145224	ARHGAP4
BrS patient 1	-	-	-	-
BrS patient 2	dup	Chr9:2,407,101-2,618,969	211869	VLDLR-AS1
	del	Chr10:68,196,544-68,517,908	321365	CTNNA3
	del	Chr11:90,802,950-90,926,931	123982	
	del	Chr16:32,564,812-32,959,259	394448	SLC6A10P
	del	ChrX:7,564,428-7,736,547	172120	

Del = deletion, dup = duplication

Table S2. Differentiation efficiency based on immunofluorescence staining for cACT (comparison experiment).

	Protocol A	Efficiency	Protocol B	Efficiency
	Dissociated iPSC-CMs		Dissociated iPSC-CMs	
Control 1	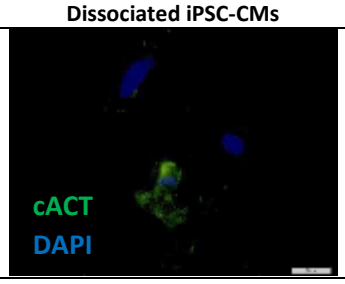	80%	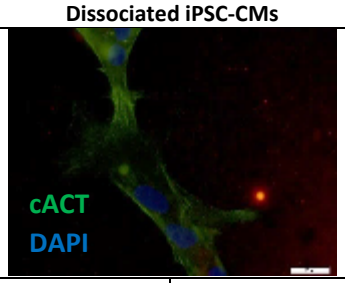	100%
	Non-dissociated monolayer		Non-dissociated monolayer	Non-dissociated monolayer
Control 2	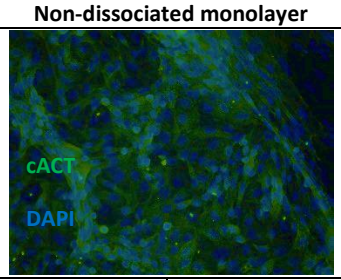	89.5 %	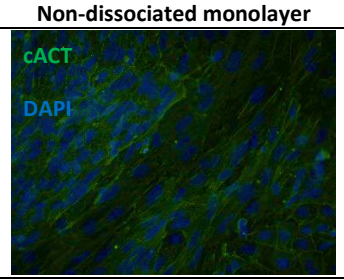	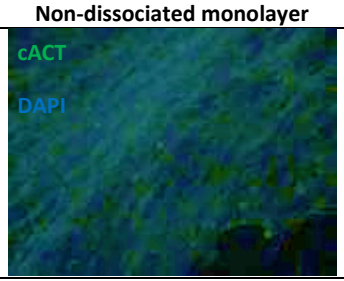 83.65 %
	Non-dissociated monolayer / Dissociated iPSC-CMs		Non-dissociated monolayer	Dissociated iPSC-CMs
BrS patient 1	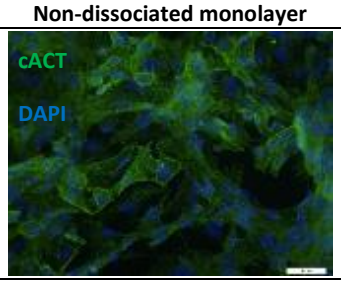 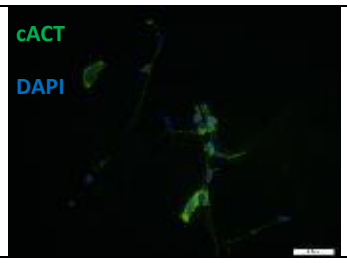	91.2 %	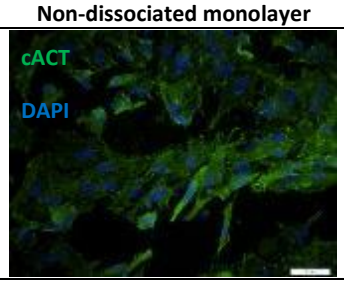	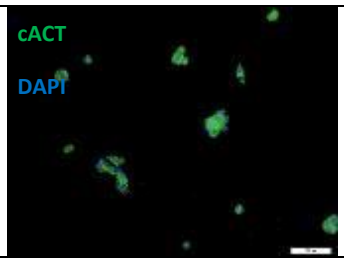 100 %
	Dissociated iPSC-CMs		Dissociated iPSC-CMs	
BrS patient 2	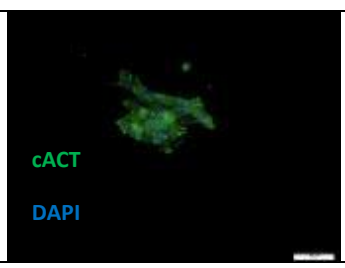	100 %	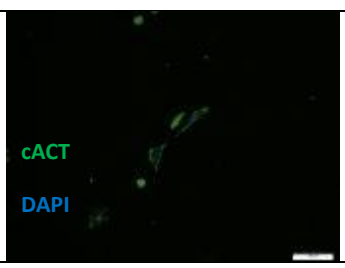	100 %

Table S3. Calculated p values for the tested cardiac markers for qPCR data on samples from the comparison between the two protocols and in relation to the reference tissue (left ventricle of a healthy human heart donor).

Tested gene	Protocol A vs. Protocol B	Protocol A/B vs. reference tissue		
	Comparison round	Comparison experiment		Validation experiment
		Protocol A	Protocol B	Protocol B
ANK2	0.155	0.059	0.414	0.323
ANK3	0.985	0.505	0.652	$1.7*E^{-6}*$
CACNA1C	0.349	0.087	0.699	0.115
GJA1	$7.5*E^{-5}*$	$3.6*E^{-5}*$	0.239	0.6
HCN4	0.453	0.439	0.776	$4.6*E^{-6}*$
KCND3	0.057	$1*E^{-6}*`$	$2.2*E^{-6}*$	$1.1*E^{-9}*$
KCNH2	0.570	0.010*	0.539	0.176
KCNJ2	$7.8*E^{-4}*$	$8.9*E^{-5}*$	0.983	0.413
KCNJ8	0.288	$1.1*E^{-16}*$	0.081	0.504
KCNQ1	0.491	$5.2*E^{-6}*$	0.002*	0.027*
MYH6	0.105	0.016*	0.013*	0.285
MYH7	0.015*	0.002*	0.171	0.539
RYR2	0.042*	$2.\ 8*E^{-6}*$	$9.9*E^{-4}*$	$4.87*E^{-5}*$
TNNI3	0.026*	$5.6*E^{-7}*$	0.0023*	0.035*
TNNT2	0.138	$1.7*E^{-4}*$	0.037*	0.175

P-values were corrected for multiple testing using Tukey's correction. *p≤0.05

Table S4. Action potential properties for iPSC-CMs generated in the comparison experiment.

Used protocol	Protocol A			Protocol B		
Cell line	Control 2	BrS patient 1	BrS patient 2	Control 2	BrS patient 1	BrS patient 2
Number of AP recordings	4	8	8	10	9	13
Number of analysed AP recordings	0^{*}	$0^{*/\dagger}$	1	$0^{*/\ddagger}$	4	2
APD50 [ms]	-	-	422.08	-	351.51± 24.84	273.7± 40.83
APD90 [ms]	-	-	501.8	-	509.95± 27.91	422.3± 10.9
APA [mV]	-	-	114.5	-	90.8± 5.1	86.7± 17.3
RMP [mV]	-	-	-59.3	-	-59.6± 3.1	-58.3± 5.4
BPM	-	-	8	-	17± 1.12	27± 3

*Recordings with RMP >-40 mV; †Recordings with proper RMP but cells did not fire AP; ‡Declined seal quality due to vivid beating

**No proper recordings were obtained from Control 1 for both tested protocols.

Table S5. Action potential and calcium transient properties for iPSC-CMs generated in validation experiment.

	Protocol B		
	Control 2	**BrS patient 1**	**BrS patient 2**
Number of analysed AP recordings	4	0	7
APD50 [ms]	617.2± 54.5	-	260.7± 59
APD90 [ms]	767.6± 56.4	-	371.5± 72.3
APA [mV]	93.9± 8.4	-	94± 4
RMP [mV]	-56.3± 3.4	-	-60.9± 4.1
BPM	21± 1	-	11± 0.3
Number of analysed CT recordings	9	11	0
CTD50 [ms]	1305.3± 41.9	389.7± 36.5	-
CTD70 [ms]	1988.9± 65.6	571.7± 52.1	-
BD [s]	6.62± 0.31	3.53± 0.06	-
BPM	9± 0.4	17± 0.3	-
Rise time [ms]	824.3± 24.6	202.3± 17.9	-
RC [ms]	1108.1± 43.4	380.3± 28.9	-

Table S6. Previously reported AP properties from commercial iPSC-CMs and iPSC-CMs differentiated using monolayer-based protocols

Reference	**Differentiation protocol**	**Culture duration**	**Patching temperature**	**AP parameters**				
				RMP	**APA**	**APD50**	**APD90**	**n**
Bett et. al. (2013)[1]	Commercial iCell CMs		RT	-63±5.8	83±11		955±103	25
Gibson et.al. (2014) [2]	Commercial iCell CMs		RT	-68±9	103±9		427±65	8
Meijer Van Puten et. al. (2015) [3]	Monolayer-based with CHIR 99021 and IWP4	30 days	36±1	-56±4	73±9		162±27	9
Lopez-Redondo et. al. (2016) [4]	Commercial iCell CMs		36±1	-43.3±1.7	79.4±2.9	309.4±29.5		54
Jeziorowska et. al. (2016) [5]	Monolayer-based using CHIR99021 and IWP2/IWR1	28-35 days	37	-69.5±9.5	96.6±15.5	586.8±404.3	726±489.6	156
Herron et. al. (2016) [6]	Commercial iCell CMs		37	-59.3±1.7	105±5			6
Feaster et. al. (2016) [7]	Monolayer-based with CHIR99021 and IWR1 + B27	30-35 days	RT	-74±1	118±3	326±13	378±14	53

Table S7. Previously reported CT properties from iPSC-CMs differentiated using monolayer-based protocols.

Reference	Differentiation protocol	Culture duration	Imaging temperature	CT parameters				
				CTD90 [ms]	CTD50 [ms]	Rise time [ms]	Decay [ms]	n
Paci et. al. (2020) [8]	Commercial iCell^2 CMs		21±1	1826.2±1071.3	920.1±456.3			42
Shah et. al. (2020) [9]	END-2 co-culture	30 days	36±1	1900±100		480±20	250±20	68
Shah et. al. (2019) [10]	END-2 co-culture	30 days	36±1			251±29	2261±676	34
Higgins et. al. (2019) [11]	Monolayer-based with CHIR99021 and IWP2	60 days	36±1		1533±100		2790±50	200
Ahola et. al. (2017) [12]	END-2 co-culture	Not specified	36±1	1663±570	797±227			13
Liang et. al. (2016) [13]	Monolayer-based with CHIR99021 and IWR1	40-60 days	36±1		471.3±12.6	92±6.6		10-25

Table S8. Immunofluorescence blocking buffers and dilutions of used antibodies for pluripotency markers

Blocking buffer	PBS (Life Technologies)	Goat serum (Jackson Immunotechnologies; 5%)		
Primary antibodies	Nanog (PA1-097, Life Technologies; dilution 1:500)	Tra1-81 (4745S, Cell Signaling Technology dilution 1:200)	Oct3/4 (sc-9081, SantaCruz Biotechnology dilution 1:100)	Tra1-60 (4746S, Cell Signaling Technology dilution 1:200)
Matching secondary antibody	Goat anti-rabbit Alexa Fluor 488 (A-11034, Life Technologies; dilution 1:500)	Goat anti-mouse (IgM) Alexa Fluor 555 (A-21426, Life Technologies; dilution 1:500)	Goat anti-rabbit Alexa Fluor 488 (A-11034, Life Technologies; dilution 1:500)	Goat anti-mouse (IgM) Alexa Fluor 555 (A-21426, Life Technologies; dilution 1:500)

Table S9. Immunofluorescence blocking buffer and dilutions of used antibodies for cardiac markers.

Blocking buffer CM markers	Goat serum (Jackson Immunotechnologies; 5%)	PBS (Life Technologies)	
Primary antibodies	Cardiac α-actinin (Abcam; dilution 1:300)	Cardiac troponin I (Abcam; dilution 1:100)	Nkx2.5 (Abcam; dilution 1:200)
Matching secondary antibodies	Goat anti rabbit (Life Technologies; dilution 1:500)	Goat anti rabbit (Life Technologies; dilution 1:500)	Goat anti mouse IgG (Life Technologies; dilution 1:500)

Table S10. Sendai vectors presence test - PCR reaction protocol

Initialization	94°C	5 min	
Denaturation	94°C	15 sec	34x
Annealing	60°C	30 sec	
Elongation	72°C	45 sec	
Final elongation	72°C	10 min	
Final hold	10°C	1 min	

Table S11. Cardiac markers qPCR primers

	FORWARD 5'-3'	REVERSE 5'-3'
REFERENCE GENES		
GAPDH	TGCACCACCAACTGCTTAGC	GGCATGGACTGTGGTCATGAG
ECHS1	AAGGCCCTCAATGCACTTTG	ACTCAGGTTCTGCATTTCCTTG
RPL13A	CCTGGAGGAGAAGAGGAAAGAGA	TTGAGGACCTCTGTGTATTTGTCAA
TARGET GENES		
ANK2	TGGACTTCACAGCCAGGAAT	GCCTCGATCCAGTAAGAGCT
ANK3	ACCAAAGGAGGACAGCAACT	GAAAAGACAGACGACCACAGG
CACNA1C	TGACATCGAGGGAGAAAACT	ACATTAGACTTGACTGCGGC
GJA1 (CX43)	GGTGACTGGAGCGCCTTAG	GCGCACATGAGAGATTGGGA
HCN4	ACCCATGCTACAGGACTTCC	GAAGAGCGCGTAGGAGTACT
KCND3	AAACAATCACAGGGACTGGC	ACACCATTGTCACCATGACC
KCNH2	TCCTTCTCCATCACCACCTC	AAATCGCCTTCTACCGGAAA
KCNJ2	GTGCGAACCAACCGCTACA	CCAGCGAATGTCCACACAC
KCNJ8	AGTGGAATGGAGAAAAGTGGT	TCCTCTGTCATCATCCTCCC
KCNQ1	ACAAAGTACTGCATGCGTCG	CATGAGAACCAACAGCTTCG
MYH6	GATAGAGAGACTCCTGCGGC	CCGTCTTCCCATTCTCGGTT
MYH7	TCGTGCCTGATGACAAACAGGAGT	ATACTCGGTCTCGGCAGTGACTTT
RYR2	CATCGAACACTCCTCTACGGA	GGACACGCTAACTAAGATGAGGT
TNNI3	TGTGGACAAGGTGGATGAAG	CCGCTTAAACTTGCCTCGAA
TNNT2	GGAGGAGCTCGTTTCTCTCA	CCTCCTGTTCTCCTCCTCCT

[1] G.C. Bett, A.D. Kaplan, A. Lis, T.R. Cimato, E.S. Tzanakakis, Q. Zhou, M.J. Morales, and R.L. Rasmusson, Electronic "expression" of the inward rectifier in cardiocytes derived from human-induced pluripotent stem cells. Heart Rhythm 10 (2013) 1903-10.

[2] J.K. Gibson, Y. Yue, J. Bronson, C. Palmer, and R. Numann, Human stem cell-derived cardiomyocytes detect drug-mediated changes in action potentials and ion currents. J Pharmacol Toxicol Methods 70 (2014) 255-67.

[3] R.M. Meijer van Putten, I. Mengarelli, K. Guan, J.G. Zegers, A.C. van Ginneken, A.O. Verkerk, and R. Wilders, Ion channelopathies in human induced pluripotent stem cell derived cardiomyocytes: a dynamic clamp study with virtual IK1. Front Physiol 6 (2015) 7.

[4] F. Lopez-Redondo, J. Kurokawa, F. Nomura, T. Kaneko, T. Hamada, T. Furukawa, and K. Yasuda, A distribution analysis of action potential parameters obtained from patch-clamped human stem cell-derived cardiomyocytes. J Pharmacol Sci 131 (2016) 141-5.

[5] D. Jeziorowska, V. Fontaine, C. Jouve, E. Villard, S. Dussaud, D. Akbar, V. Letang, P. Cervello, J.M. Itier, M.P. Pruniaux, and J.S. Hulot, Differential Sarcomere and Electrophysiological Maturation of Human iPSC-Derived Cardiac Myocytes in Monolayer vs. Aggregation-Based Differentiation Protocols. Int J Mol Sci 18 (2017).

[6] T.J. Herron, A.M. Rocha, K.F. Campbell, D. Ponce-Balbuena, B.C. Willis, G. Guerrero-Serna, Q. Liu, M. Klos, H. Musa, M. Zarzoso, A. Bizy, J. Furness, J. Anumonwo, S. Mironov, and J. Jalife, Extracellular Matrix-Mediated Maturation of Human Pluripotent Stem Cell-Derived Cardiac Monolayer Structure and Electrophysiological Function. Circ Arrhythm Electrophysiol 9 (2016) e003638.

[7] T.K. Feaster, A.G. Cadar, L. Wang, C.H. Williams, Y.W. Chun, J.E. Hempel, N. Bloodworth, W.D. Merryman, C.C. Lim, J.C. Wu, B.C. Knollmann, and C.C. Hong, Matrigel Mattress: A Method for the Generation of Single Contracting Human-Induced Pluripotent Stem Cell-Derived Cardiomyocytes. Circ Res 117 (2015) 995-1000.

[8] M. Paci, E. Passini, A. Klimas, S. Severi, J. Hyttinen, B. Rodriguez, and E. Entcheva, All-Optical Electrophysiology Refines Populations of In Silico Human iPSC-CMs for Drug Evaluation. Biophys J 118 (2020) 2596-2611.

[9] D. Shah, C. Prajapati, K. Penttinen, R.M. Cherian, J.T. Koivumaki, A. Alexanova, J. Hyttinen, and K. Aalto-Setala, hiPSC-Derived Cardiomyocyte Model of LQT2 Syndrome Derived from Asymptomatic and Symptomatic Mutation Carriers Reproduces Clinical Differences in Aggregates but Not in Single Cells. Cells 9 (2020).

[10] D. Shah, L. Virtanen, C. Prajapati, M. Kiamehr, J. Gullmets, G. West, J. Kreutzer, M. Pekkanen-Mattila, T. Helio, P. Kallio, P. Taimen, and K. Aalto-Setala, Modeling of LMNA-Related Dilated Cardiomyopathy Using Human Induced Pluripotent Stem Cells. Cells 8 (2019).

[11] E.M. Higgins, J.M. Bos, S.M. Dotzler, C.S. John Kim, and M.J. Ackerman, MRAS Variants Cause Cardiomyocyte Hypertrophy in Patient-Specific Induced Pluripotent Stem Cell-Derived Cardiomyocytes: Additional Evidence for MRAS as a Definitive Noonan Syndrome-Susceptibility Gene. Circ Genom Precis Med 12 (2019) e002648.

[12] A. Ahola, R.P. Polonen, K. Aalto-Setala, and J. Hyttinen, Simultaneous Measurement of Contraction and Calcium Transients in Stem Cell Derived Cardiomyocytes. Ann Biomed Eng 46 (2018) 148-158.

[13] P. Liang, K. Sallam, H. Wu, Y. Li, I. Itzhaki, P. Garg, Y. Zhang, V. Vermglinchan, F. Lan, M. Gu, T. Gong, Y. Zhuge, C. He, A.D. Ebert, V. Sanchez-Freire, J. Churko, S. Hu, A. Sharma, C.K. Lam, M.M. Scheinman, D.M. Bers, and J.C. Wu, Patient-Specific and Genome-Edited Induced Pluripotent Stem Cell-Derived Cardiomyocytes Elucidate Single-Cell Phenotype of Brugada Syndrome. J Am Coll Cardiol 68 (2016) 2086-2096.